Editors' Suggestion | Featured in Physics

Improved Isotope-Shift-Based Bounds on Bosons beyond the Standard Model through Measurements of the $^2D_{3/2} - {}^2D_{5/2}$ Interval in Ca^+

Cyrille Solaro,[1,*] Steffen Meyer,[1,†] Karin Fisher,[1] Julian C. Berengut,[2,‡] Elina Fuchs,[3,4,§] and Michael Drewsen[1,‖]

[1]*Department of Physics and Astronomy, Aarhus University, DK-8000 Aarhus C, Denmark*
[2]*School of Physics, University of New South Wales, Sydney, New South Wales 2052, Australia*
[3]*Theory Department, Fermilab, Batavia, Illinois 60510, USA*
[4]*Department of Physics, University of Chicago, Chicago, Illinois 60637, USA*

(Received 1 May 2020; accepted 20 August 2020; published 15 September 2020)

We perform high-resolution spectroscopy of the $3d\,^2D_{3/2} - 3d\,^2D_{5/2}$ interval in all stable even isotopes of $^A Ca^+$ ($A = 40$, 42, 44, 46, and 48) with an accuracy of ~20 Hz using direct frequency-comb Raman spectroscopy. Combining these data with isotope shift measurements of the $4s\,^2S_{1/2} \leftrightarrow 3d\,^2D_{5/2}$ transition, we carry out a King plot analysis with unprecedented sensitivity to coupling between electrons and neutrons by bosons beyond the standard model. Furthermore, we estimate the sensitivity to such bosons from equivalent spectroscopy in Ba^+ and Yb^+. Finally, the data yield isotope shifts of the $4s\,^2S_{1/2} \leftrightarrow 3d\,^2D_{3/2}$ transition at 10 parts per billion through combination with recent data of Knollmann, Patel, and Doret [Phys. Rev. A **100**, 022514 (2019)].

DOI: 10.1103/PhysRevLett.125.123003

The standard model of particle physics (SM) cannot be complete, since, e.g., it lacks a dark matter candidate, cannot produce the observed matter-antimatter asymmetry of the Universe, and does not explain the hierarchy between the Higgs mass and the Planck scale. Because the masses of new particles are unknown, searches for new physics (NP) beyond the SM involve multiple frontiers (see, e.g., Refs. [1–3], and references therein) ranging from high-energy colliders, high-intensity beam dumps, and astrophysical and cosmological observations to high-precision tabletop experiments. In the search for new long-range interactions, high-resolution spectroscopy of atoms and molecules is a driving force [4]. A recent example is to probe the existence of new bosons that couple to both nucleons and electrons from precisely measured isotope shifts. Conversely, agreement between the prediction based on the SM and experiments within their uncertainties allows for placing bounds on the coupling strength of the potential new interaction depending on the mass of the new boson. Except for few-electron systems [5], the main limitation in translating the experimental accuracy to a stringent bound is the theory uncertainty. To mitigate this problem, Delaunay *et al.* [6] proposed to measure isotope shifts of two different transitions of the same element and to look for a nonlinearity of the so-called King plot [7]. This allows one to place bounds on long-range mediators [8] and, thus, to test various particle physics models [9]. For instance, the protophobic model [10,11] of a new boson at 17 MeV/c^2 for the Be anomaly [12] is in reach of near-future Sr/Sr^+ and Yb^+ King plot analyses [8,9]. This data-driven method requires only theory input for the new interaction but is independent of SM multielectron and nuclear calculations—unless a nonlinearity from higher-order SM effects is predicted at the level of experimental precision. After subtracting the predicted SM nonlinearity, the residual nonlinearity can be used to constrain a NP contribution. A King plot, however, requires at least four isotopes (preferably with zero nuclear spin) in order to test the linearity of the isotope shifts of the resulting three independent isotope pairs. Calcium is in this respect a good candidate with the five stable, spin-0 isotopes $A = 40$, 42, 44, 46, and 48. Previously, Gebert *et al.* reported measurements of two dipole-allowed transitions, $4s\,^2S_{1/2} \leftrightarrow 4p\,^2P_{1/2}$ (397 nm) and $3d\,^2D_{3/2} \leftrightarrow 4p\,^2P_{1/2}$ (866 nm), in the four $^{40,42,44,48}Ca^+$ isotopes with an accuracy of $\mathcal{O}(100)$ kHz corresponding to a fractional accuracy on the isotope shifts in the 10^{-5}–10^{-4} range [13]. In principle, far better accuracy can be achieved on narrow-optical transitions [14] such as the two $4s$-$3d$ quadrupole transitions. While the $4s\,^2S_{1/2} \leftrightarrow 3d\,^2D_{5/2}$ (729-nm) transition has been measured at the 10-mHz level in $^{40}Ca^+$ [15,16], measurement of the $4s\,^2S_{1/2} \leftrightarrow 3d\,^2D_{3/2}$ (732-nm) transition at the same level is more challenging, since the electron-shelving technique [17] cannot directly be used for state detection.

In this Letter, we report isotope shift measurements of the $3d\,^2D_{3/2} - 3d\,^2D_{5/2}$ interval [i.e., the D-fine-structure splitting isotope shift (DSIS)] on all five stable even isotopes of $^A Ca^+$ (with $A = 40$ as the reference isotope) using direct frequency-comb Raman spectroscopy [18]. Combining these with isotope shift measurements of the $4s\,^2S_{1/2} \leftrightarrow 3d\,^2D_{5/2}$ transition (729 IS), we deduce the isotope shift of the $4s\,^2S_{1/2} \leftrightarrow 3d\,^2D_{3/2}$ transition (732 IS). This leads to a King plot analysis with unprecedented sensitivity to NP bosons coupling to both electrons and neutrons. In addition, the analysis yields a field shift ratio of

TABLE I. Isotope shifts relative to $^{40}Ca^+$ in megahertz and their 1 standard deviation σ uncertainties.

A	$\delta\nu_{\mathrm{DSIS}}^{A,40}$	$\delta\nu_{729}^{A,40}$	$\delta\nu_{732}^{A,40}$ [c]
42	−3.519896(24) [a]	2771.873(2) [a]	2775.393(2) [a]
		2771.872 467 6(76) [b]	2775.392 363(25) [d]
44	−6.792470(22) [a]	5340.888(2) [a]	5347.680(2) [a]
		5340.887 394 6(78) [b]	5347.679 865(23) [d]
46	−9.901524(21) [a]	7768.401(2) [a]	7778.302(2) [a]
48	−12.746610(27) [a]	9990.383(2) [a]	10 003.130(2) [a]
		9990.381 870 0(63) [b]	10 003.128 480(28) [d]

[a]This work.
[b]Taken from Ref. [19].
[c]Calculated: $\delta\nu_{732}^{A,40} = \delta\nu_{729}^{A,40} - \delta\nu_{\mathrm{DSIS}}^{A,40}$.
[d]Calculated using values of $\delta\nu_{729}^{A,40}$ from Ref. [19].

the 729- and 732-nm transitions with an unprecedented fractional accuracy of 2×10^{-7}. We achieve an absolute accuracy on the DSIS at the 20-Hz level corresponding to a fractional accuracy in the 10^{-6} range, and on the 729 IS at the 2-kHz level corresponding to a fractional accuracy in the 10^{-7} range. We show that, with respect to bounds on NP bosons, our measurements are, in fact, equally precise as measuring the isotope shift of the two $4s$-$3d$ transitions with the same 20-Hz level accuracy, since the limiting fractional accuracy is the DSIS measurement. In particular, the King plot analysis is not improved through combination with recent 729-IS measurements at the 10^{-9} level by Knollmann, Patel, and Doret [19]. It is neither limited by the 729 IS involving the isotope $^{46}Ca^+$ that was not measured in Ref. [19]. However, the combined data yield isotope shifts of the 732-nm transition with fractional accuracy below the 10^{-8} level.

The splitting isotope shift of the $3d\,^2D_{3/2}$ and $3d\,^2D_{5/2}$ states $\delta\nu_{\mathrm{DSIS}}^{A,40}$ was measured using direct frequency-comb Raman spectroscopy, as described in detail in Ref. [18]. In brief, a single Ca^+ isotope is loaded into a linear Paul trap via isotope-selective photoionization in a neutral calcium beam [20,21]. An external magnetic field of 6.500(3) G lifts the Zeeman degeneracy of the involved electronic energy levels by a few MHz, allowing for Zeeman-resolved spectroscopy of the $D_{3/2}$-$D_{5/2}$ interval. The experimental cycle is initialized by Doppler cooling, followed by sideband cooling and finally optical pumping of the Ca^+ ion into one of its $|4s\,^2S_{1/2}, m_j = \pm 1/2\rangle$ states. Next, the ion is transfered to the $|D_{5/2}, m_j = \pm 1/2\rangle$ state using rapid adiabatic passage [22,23]. Finally, direct frequency-comb Raman spectroscopy of the two $|D_{5/2}, m_j = \pm 1/2\rangle \leftrightarrow |D_{3/2}, m_j' = \pm 1/2\rangle$ symmetric transitions is carried out [18]. The state of the ion is read out by the electron-shelving technique [17]. The first-order differential Zeeman shift induced by the static magnetic field is canceled by averaging the two transition frequencies. The differential ac-Stark shift induced by the frequency comb is reduced by taking advantage of the existence of a "magic polarization" [18], and the unshifted transition frequency is obtained by extrapolating the measured frequencies to zero light intensity. The measured absolute D-splitting isotope shifts $\delta\nu_{\mathrm{DSIS}}^{A,40}$ corrected for systematic effects (i.e., second-order Zeeman shift and electric-quadrupole shift mainly [18]) are presented Table I. The achieved relative accuracy ranges from 2 to 7×10^{-6}.

The $4s\,^2S_{1/2} \leftrightarrow 3d\,^2D_{5/2}$ transition near 729 nm was measured by Rabi spectroscopy [24]. In an experimental sequence similar to the one described above, after the optical pumping stage, the two $|S_{1/2}, \pm 1/2\rangle \leftrightarrow |D_{5/2}, \mp 3/2\rangle$ transitions are probed consecutively with π-pulses. The interrogation laser is locked to an ultrastable high-finesse cavity providing a subkilohertz linewidth at short term (see Fig. 1). The absolute laser frequency is measured

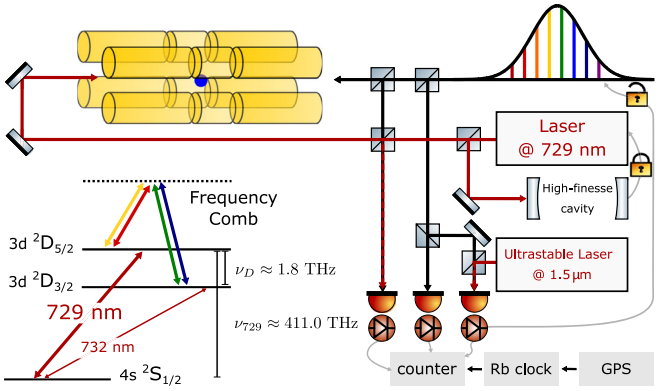

FIG. 1. Schematic of the experimental setup and the relevant electronic levels of the Ca^+ ion. The isotope shift of the 732-nm transition can be deduced from the isotope shifts of the 729-nm transition and of the D-fine-structure splitting. The D-fine-structure splitting is measured successively on the different calcium isotopes by direct frequency-comb Raman spectroscopy [18]. The transition frequency is deduced from the measurement of the comb repetition rate on a frequency counter referenced to a GPS-disciplined rubidium standard. The 729-nm laser used to probe the $4s\,^2S_{1/2} \leftrightarrow 3d\,^2D_{5/2}$ transition is locked to an ultrastable high-finesse cavity providing a short-term linewidth < 1 kHz. The absolute laser frequency is deduced from a measurement on the frequency counter of the beating between the laser and the frequency comb with the latter locked to an ultrastable laser at 1.5 μm.

by beating this laser with one tooth of the frequency comb with the latter locked to an acetylene-stabilized ultrastable fiber laser (*Stabiλaser* from Denmark's National Metrology Institute [25,26]). The differential first-order Zeeman shift is once again canceled by averaging the two transition frequencies. These measurements are limited by the relative inaccuracy of our GPS-disciplined rubidium standard which was measured against the *Stabiλaser* to be 5×10^{-12}. This corresponds to a 2-kHz accuracy on the $S_{1/2}$-$D_{5/2}$ transition and a relative accuracy on $\delta\nu_{729}^{A,40}$ ranging from 2 to 7×10^{-7}. The deduced isotope shifts $\delta\nu_{729}^{A,40}$ are given Table I together with parts-per-billion measurements of $\delta\nu_{729}^{42,44,48-40}$ reported by Knollmann, Patel, and Doret [19]. Combined with our DSIS measurements, the data of Ref. [19] are further used to calculate the isotope shifts of the $4s\,^2S_{1/2} \leftrightarrow 3d\,^2D_{3/2}$ transition near 732 nm with a fractional accuracy better than 10^{-8}, as also presented in Table I.

The two leading contributions to the isotope shift in atomic transition frequencies are the mass shift (MS) and the field shift (FS) [27]. The MS originates from the difference of the nuclear mass which leads to differences in the nuclear recoil energy. The FS originates from the change in the effective nuclear charge radius, which leads to different electronic potentials near the origin. With these two contributions, the isotope shift of a transition i in A with respect to A' can to leading order be written as:

$$\delta\nu_i^{AA'} \equiv \nu_i^A - \nu_i^{A'} = \delta\nu_{i,\mathrm{MS}}^{AA'} + \delta\nu_{i,\mathrm{FS}}^{AA'} = \frac{K_i}{\mu} + F_i \delta\langle r_c^2\rangle^{AA'}, \quad (1)$$

where K_i and F_i are the mass and field shift constants, respectively, $\delta\langle r_c^2\rangle^{AA'} = \langle r_c^2\rangle^A - \langle r_c^2\rangle^{A'}$ is the difference of the mean squared nuclear charge radii, and μ is the relative mass change given by [28]

$$\mu = \mu^{AA'} = \frac{m_{A'}(m_A + m_e)}{m_A - m_{A'}}, \quad (2)$$

where m_e is the electron mass and m_A and $m_{A'}$ are the masses of the *nuclei* of the two isotopes, respectively. The nuclear masses can be deduced from the precisely determined masses of the neutral atomic calcium isotopes [29], the total mass of the electrons, and the sum of the electrons binding energies E_n^b:

$$m_A = m_{A,\text{neutral atom}} - 20m_e + \sum_{n=1}^{20} E_n^b, \quad (3)$$

where the electron binding energies have been extracted from the NIST database [30]. If the isotope shifts are measured for more than one transition, Eq. (1) allows one to eliminate the typically poorly known $\delta\langle r_c^2\rangle^{AA'}$ and to write the so-called King relation [7]:

$$\mu\delta\nu_i^{AA'} = K_i - \frac{F_i}{F_j}K_j + \frac{F_i}{F_j}\mu\delta\nu_j^{AA'}, \quad (4)$$

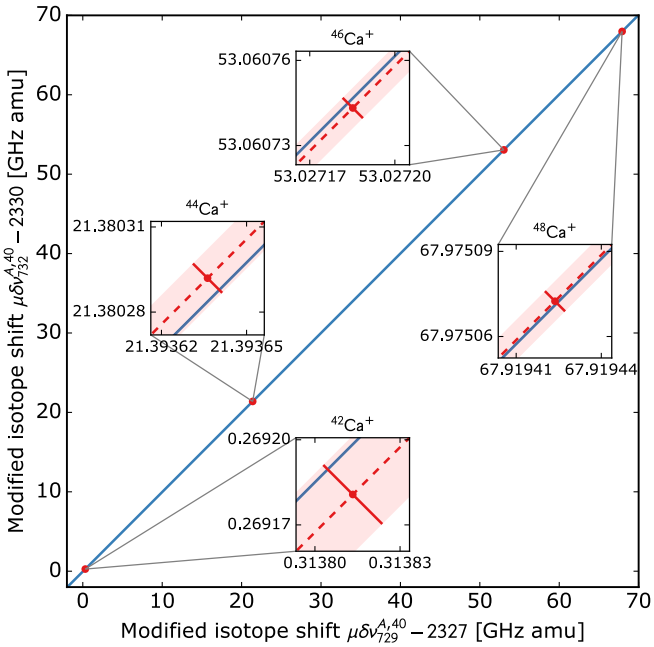

FIG. 2. Two-dimensional King plot of the 732- and 729-nm transitions. The line is a fit to our data using a weighted orthogonal distance regression. The extracted fit parameters are given in the text. We point out that the isotope shift of the 732-nm transition is deduced from measurements of the isotope shift of the 729-nm transition $\delta\nu_{729}^{A,40}$ and of the D-splitting isotope shift $\delta\nu_{\mathrm{DSIS}}^{A,40}$. Hence, the measurement accuracy on $\delta\nu_{729}^{A,40}$ ($\delta\nu_{\mathrm{DSIS}}^{A,40}$) translates into an error bar parallel (perpendicular) to the fitted line, emphasizing that the analysis is limited by the achieved fractional accuracy on $\delta\nu_{\mathrm{DSIS}}^{A,40}$.

which, to leading order within the SM, is a linear relation between the modified isotope shifts $\mu\delta\nu_i^{AA'}$ and $\mu\delta\nu_j^{AA'}$ of the two transitions i and j. A NP interaction mediated by a boson ϕ of spin s with coupling strengths y_e and y_n to electrons and neutrons, respectively, modifies the isotope shift predictions of Eq. (1) as [8]

$$\delta\nu_i^{AA'} = \frac{K_i}{\mu} + F_i\delta\langle r_c^2\rangle^{AA'} + (-1)^s \frac{\hbar c}{4\pi}\frac{y_e y_n}{\hbar c} X_i \gamma^{AA'}, \quad (5)$$

where the electronic NP coefficient X_i characterizes the overlap of the wave functions of the lower and upper states of transition i with the potential mediated by the boson, independent of the isotopes, and $\gamma^{AA'}$ depends on the isotopes only, independent of the transition. If ϕ couples linearly to the nucleus, then $\gamma^{AA'} = A - A'$. As a consequence, the King relation in Eq. (4) is in this case not linear anymore. Therefore, searching for nonlinearities of the corresponding King plot provides sensitivity to a NP interaction mediated by such a boson.

The King plot of the modified isotope shift of the $i = 732$ nm transition against the modified isotope shift of the $j = 729$ nm transition, using our experimental data only, is shown in Fig. 2. The blue line is a linear fit of the data using the King relation Eq. (4) and a weighted orthogonal

distance regression [31]. The error bars represent the 1σ uncertainties which are limited by our measurement accuracy and not by the uncertainty on the isotope masses (see Supplemental Material [32] for details). We emphasize that $\delta\nu^{A,40}_{732}$ is deduced from measurements of $\delta\nu^{A,40}_{729}$ and $\delta\nu^{A,40}_{\mathrm{DSIS}}$ and that $\delta\nu^{A,40}_{729} \gg \delta\nu^{A,40}_{\mathrm{DSIS}}$. Consequently, the measurement uncertainties on $\delta\nu^{A,40}_{729}$ and $\delta\nu^{A,40}_{\mathrm{DSIS}}$ translate into error bars essentially parallel and perpendicular to the fitted line, illustrating that the analysis is limited nearly exclusively by the achieved accuracy on $\delta\nu^{A,40}_{\mathrm{DSIS}}$. In fact, as long as the fractional accuracy on $\delta\nu^{A,40}_{729}$ is smaller than the fractional accuracy on $\delta\nu^{A,40}_{\mathrm{DSIS}}$, measuring the DSIS at, e.g., the 20-Hz level is equivalent to measuring both the 729 IS and the 732 IS with the same 20-Hz accuracy. This is a consequence of the King plot analysis being sensitive to the difference of isotope shifts of the $D_{3/2}$ and $D_{5/2}$ states, and this demonstrates the potential of measuring the DSIS directly using direct frequency-comb Raman spectroscopy.

The reduced χ^2 of the fit is 0.89, and the King plot is thus linear within our measurement uncertainty. The nonlinearity (defined in Supplemental Material [32]) is 1.26σ. This allows for translating our measurement uncertainty into a constraint on the coupling strength of a hypothetical boson ϕ. For a Yukawa potential $V_{\mathrm{NP}} = (-1)^s(A-Z)(\hbar c/4\pi)\times(y_e y_n/\hbar c)(e^{-r m_\phi c/\hbar}/r)$, where Z is the number of protons, we calculate the electronic NP coefficients X_i using Brueckner orbitals and including relativistic random phase approximation corrections to the operator (see [32]). By constraining the nonlinear term from data (see [8,32]) and using the theory calculation of X_i, we evaluate the bounds on $y_e y_n$ as a function of a potential new mediator's mass m_ϕ which are shown in Fig. 3. The red solid curve corresponds to the bound using our experimental data only, yielding $y_e y_n/\hbar c < 6.9\times10^{-11}$ at the 2σ level in the massless limit ($m_\phi = 1$ eV). The combination of the 729-IS measurements of Ref. [19] with our measurements of the DSIS and of $\delta\nu^{40,46}_{729}$, however, does not improve the bound despite the thousand times better accuracy on $\delta\nu^{42,44,48-40}_{729}$, confirming that the accuracy on the DSIS is the limiting one (as long as $\sigma_{S-D_{5/2}}\cdot F_{\mathrm{DSIS}}/F_{S-D_{5/2}} < \sigma_{\mathrm{DSIS}}$) and illustrating the potential of measuring the DSIS directly. The combined bound coincides with the bound using purely our data (up to a relative difference of 1%) and is therefore not displayed. The black curve corresponds to the previous best bound set by measurements of the isotope shift of the two $S_{1/2}$-$P_{1/2}$ and $D_{3/2}$-$P_{1/2}$ dipole-allowed transitions by Gebert *et al.* [13] limiting $y_e y_n/\hbar c < 2\times10^{-9}$ for $m_\phi = 0$. We note that, despite the hundred times better relative accuracy on the two $4s$-$3d$ transition isotope shifts achieved in this work, the bounds on $y_e y_n$ are improved by less than a factor 100. This is because the electronic configurations of the $D_{3/2}$ and $D_{5/2}$ states are more similar than the ones of the relevant $S_{1/2}$ and $D_{3/2}$ states of Ref. [13]. More stringent bounds could be placed by constraining King plot nonlinearities with heavier elements provided that one can correct for the nonlinearities already predicted at higher order within the SM [40]. Two promising elements are Ba^+ or Yb^+, which both have five spin-0 isotopes and D splittings of 24 and 42 THz, respectively. The projected constraints imposed by measuring the DSIS at the 20-Hz level and the $S_{1/2}$-$D_{5/2}$ transition isotope shifts at the kHz level in Ba^+ (green, dashed line) and Yb^+ (dark blue, dashed line) are also plotted in Fig. 3 (see [32]). Furthermore, we estimate the sensitivity of Ca^+, Ba^+, and Yb^+ for measurements of the DSIS with 10-mHz accuracy and of the $S_{1/2}$-$D_{5/2}$ transition isotope shifts with $\sim$ Hz accuracy, under the condition that the uncertainty is limited by the isotope shift measurements. This is reasonable, since the current uncertainty on the isotope mass

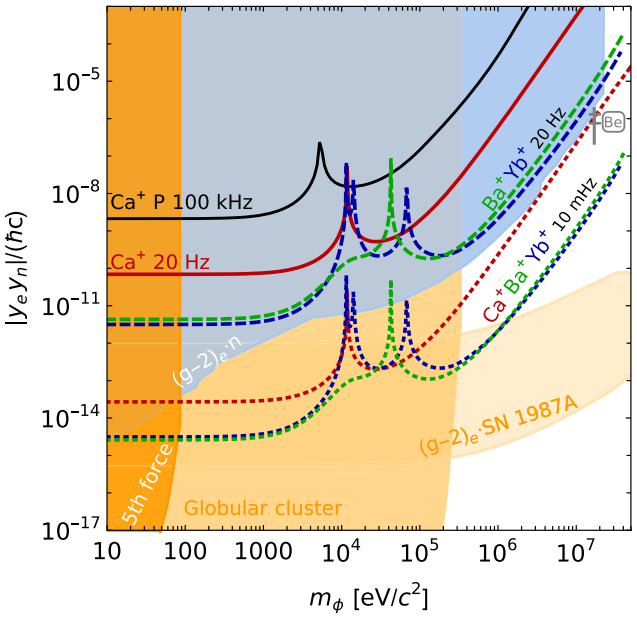

FIG. 3. Current and projected constraints (2σ) on the coupling strength $|y_e y_n|/(\hbar c)$ of electrons and neutrons to a new boson ϕ of mass m_ϕ. Existing bound [8] from measurements of the $S_{1/2}$-$P_{1/2}$ and $D_{3/2}$-$P_{1/2}$ transition isotope shifts in Ca^+ with an accuracy of $\mathcal{O}(100\ \mathrm{kHz})$ [13] (black line, labeled as P). Constraint imposed by this work (red, solid line), limited by the ~20-Hz measurement uncertainty of the DSIS. Projection for a 10-mHz uncertainty on the DSIS (red, dotted line). Projected constraints from measurements in Ba^+ (DSIS at 20-Hz level, green dashed line; 10 mHz, green dotted line) and in Yb^+ isotopes (dark blue line, also for 20 Hz and 10 mHz) (for details, see [32]). The curves end at masses m_ϕ that correspond to the inverse nuclear radii. For comparison, constraints from other experiments are shown as shaded areas [8]: fifth force [60,61] (dark orange), $(g-2)_e$ measurements [49,50] combined with neutron scattering data [51–54] (light blue), or SN 1987A (light orange), and star cooling in globular clusters [44–48] (orange). The gray bar represents the range of $y_e y_n$ to explain the Be anomaly at $m_\phi = 17$ MeV [8–12], while the part within the horizontal gray lines is the remaining allowed range with y_e between the NA64 [55] and NA48/2 [57] limits and y_n from Ref. [58] including isospin mixing and breaking.

affects the King plot linearity at a level of a few 10 mHz only (see [32]) and that measurements with a 100-times better accuracy can be performed in Penning traps [41–43]. The current constraints on $y_e y_n$ from King plot analyses, included the new bound derived in this work, are weaker than the astrophysical bound from star cooling of globular clusters [44–48] for $m_\phi \lesssim 0.3\ \mathrm{MeV}/c^2$ and weaker than the constraint on y_e from the magnetic dipole moment $(g-2)$ of the electron [49,50] combined with the constraint on y_n from neutron scattering [51–54]. In contrast, the improved accuracy of the DSIS and $S_{1/2}$-$D_{5/2}$ measurements have the potential to probe so far unconstrained parameter space for $m_\phi \gtrsim 0.3\ \mathrm{MeV}/c^2$ and, in particular, the range of $y_e y_n$ at $m_\phi = 17\ \mathrm{MeV}/c^2$ needed to explain the Be anomaly by a protophobic vector boson. Its electron coupling is constrained by the NA64 [55,56] and NA48 [57] beam dump experiments and $(g-2)_e$, while the neutron coupling is constrained by the nuclear Be decay width [58]. The requirement on the particle's lifetime to ensure its decay within the detector make the beam dump bounds on y_e model dependent. Isotope shifts, in contrast, directly constrain the coupling product $y_e y_n$ model independently. To further probe the vector model, see, e.g., other nuclear decays in Ref. [58] and constraints on the muon coupling in Ref. [59].

Finally, considering the case without a NP contribution, the fit parameters of the King plot analysis are $K_{ij} = K_{732} - F_{732}/F_{729}K_{729} = -0.4961(5)$ GHz amu and $F_{ij} = F_{732}/F_{729} = 1.00148305(20)$. Notably, we extract the ratio of the field shift constants with a relative accuracy of 2×10^{-7}, and the obtained value matches well the theoretical value calculated using many-body perturbation theory (see [32]) $F_{ij}^{\mathrm{MBPT}} = 1.0016$. We mention that this is also the case for the field shift ratio of the $S_{1/2}$-$P_{1/2}$ and $S_{1/2}$-$P_{3/2}$ transitions which isotope shifts were recently measured by Müller *et al.* [62], solving the field shift puzzle introduced with previous measurements made by Shi *et al.* [63]. Lastly, our data could be used to improve the accuracy on $\delta\langle r_c^2\rangle^{AA'}$ for the even calcium isotopes considered here [64].

In summary, we have reported measurements of the D-fine-structure splitting isotope shift using direct frequency-comb Raman spectroscopy on all stable even isotopes of $^A\mathrm{Ca}^+$ ($A = 40$, 42, 44, 46, and 48) with an accuracy of ~20 Hz. Combined with isotope shift measurements of the $4s\,^2\mathrm{S}_{1/2} \leftrightarrow 3d\,^2\mathrm{D}_{5/2}$ transition at the 2-kHz level, we performed a King plot analysis of the $4s\,^2\mathrm{S}_{1/2} \leftrightarrow 3d\,^2\mathrm{D}_{5/2}$ and $4s\,^2\mathrm{S}_{1/2} \leftrightarrow 3d\,^2\mathrm{D}_{3/2}$ transitions with unprecedented accuracy and extracted the field shift ratio with a fractional accuracy of 2×10^{-7}. Furthermore, the achieved uncertainty on the King plot linearity was used to improve isotope-shift-based bounds on the coupling strength of a new physics boson to both electrons and neutrons. More stringent bounds could be placed by looking for King plot nonlinearities with heavier elements, such as Ba^+ or Yb^+ applying direct frequency-comb Raman spectroscopy. Finally, NP interactions mediated by bosons with masses $m_\phi \gtrsim 0.3\ \mathrm{MeV}/c^2$ and so far unconstrained by experiments could be probed by measuring, with existing techniques for optical atomic clocks, the DSIS at the 10-mHz level and one of the S-D isotope shifts at the ~ Hz level.

We thank J. Hur, V. Vuletić, M. Schlaffer, R. Ozeri, P. O. Schmidt, C. Delaunay, and Y. Soreq for interesting discussions. We acknowledge the Danish Center for Laser Infrastructure, LASERLAB.DK, established through the support of the Danish Ministry of Research and Education, for financial support and access to the frequency comb. We also acknowledge support from Innovation Fund Denmark, through the Quantum Innovation Center, Qubiz, for financial support and access to the *Stabiλaser*. C. S. acknowledges support from the European Commission through the Marie Skłodowska-Curie Individual Fellowship COMAMOC (Grant Agreement No. 795107) under Horizon 2020. S. M. and K. F. acknowledge support from the European Commission through the Marie Curie Initial Training Network COMIQ (Grant Agreement No. 607491) under FP7. J. C. B. and E. F. thank the MPIK Heidelberg for hospitality that enabled important discussions in the initial phase of this work. E. F. was supported during part of this work by the Minerva Foundation and the Weizmann Institute of Science in Israel. J. C. B. is supported in this work by the Australian Research Council (DP190100974). M. D. acknowledges support from the European Commissions FET Open TEQ, the Villum Foundation, and the Sapere Aude Initiative from the Independent Research Fund Denmark.

*solaro@phys.au.dk
†steffen.meyer@phys.au.dk
‡julian.berengut@unsw.edu.au
§elinafuchs@uchicago.edu
‖drewsen@phys.au.dk

[1] M. Mangano, arXiv:2003.05976.
[2] D. Bettoni, S. Bianco, F. Bossi, M. Catanesi, A. Ceccucci, F. Cervelli, M. Dellorso, U. Dosselli, F. Ferroni, and M. Grassi, Phys. Rep. **434**, 47 (2006).
[3] D. DeMille, J. M. Doyle, and A. O. Sushkov, Science **357**, 990 (2017).
[4] M. S. Safronova, D. Budker, D. DeMille, D. F. J. Kimball, A. Derevianko, and C. W. Clark, Rev. Mod. Phys. **90**, 025008 (2018).
[5] C. Delaunay, C. Frugiuele, E. Fuchs, and Y. Soreq, Phys. Rev. D **96**, 115002 (2017).
[6] C. Delaunay, R. Ozeri, G. Perez, and Y. Soreq, Phys. Rev. D **96**, 093001 (2017).
[7] W. H. King, J. Opt. Soc. Am. **53**, 638 (1963).
[8] J. C. Berengut, D. Budker, C. Delaunay, V. V. Flambaum, C. Frugiuele, E. Fuchs, C. Grojean, R. Harnik, R. Ozeri, G. Perez, and Y. Soreq, Phys. Rev. Lett. **120**, 091801 (2018).

[9] C. Frugiuele, E. Fuchs, G. Perez, and M. Schlaffer, Phys. Rev. D **96**, 015011 (2017).
[10] J. L. Feng, B. Fornal, I. Galon, S. Gardner, J. Smolinsky, T. M. P. Tait, and P. Tanedo, Phys. Rev. Lett. **117**, 071803 (2016).
[11] J. L. Feng, B. Fornal, I. Galon, S. Gardner, J. Smolinsky, T. M. P. Tait, and P. Tanedo, Phys. Rev. D **95**, 035017 (2017).
[12] A. J. Krasznahorkay, M. Csatlós, L. Csige, Z. Gácsi, J. Gulyás, M. Hunyadi, I. Kuti, B. M. Nyakó, L. Stuhl, J. Timár, T. G. Tornyi, Z. Vajta, T. J. Ketel, and A. Krasznahorkay, Phys. Rev. Lett. **116**, 042501 (2016).
[13] F. Gebert, Y. Wan, F. Wolf, C. N. Angstmann, J. C. Berengut, and P. O. Schmidt, Phys. Rev. Lett. **115**, 053003 (2015).
[14] T. Manovitz, R. Shaniv, Y. Shapira, R. Ozeri, and N. Akerman, Phys. Rev. Lett. **123**, 203001 (2019).
[15] Y. Huang, H. Guan, P. Liu, W. Bian, L. Ma, K. Liang, T. Li, and K. Gao, Phys. Rev. Lett. **116**, 013001 (2016).
[16] Y. Huang, H. Guan, M. Zeng, L. Tang, and K. Gao, Phys. Rev. A **99**, 011401(R) (2019).
[17] H. G. Dehmelt, IEEE Trans. Instrum. Meas. **IM-31**, 83 (1982).
[18] C. Solaro, S. Meyer, K. Fisher, M. V. DePalatis, and M. Drewsen, Phys. Rev. Lett. **120**, 253601 (2018).
[19] F. W. Knollmann, A. N. Patel, and S. C. Doret, Phys. Rev. A **100**, 022514 (2019).
[20] N. Kjærgaard, L. Hornekær, A. Thommesen, Z. Videsen, and M. Drewsen, Appl. Phys. B **71**, 207 (2000).
[21] A. Mortensen, J. J. T. Lindballe, I. S. Jensen, P. Staanum, D. Voigt, and M. Drewsen, Phys. Rev. A **69**, 042502 (2004).
[22] A. Turrin, Opt. Commun. **23**, 220 (1977).
[23] C. Wunderlich, T. Hannemann, T. Körber, H. Häffner, C. Roos, W. Hänsel, R. Blatt, and F. Schmidt-Kaler, J. Mod. Opt. **54**, 1541 (2007).
[24] I. I. Rabi, S. Millman, P. Kusch, and J. R. Zacharias, Phys. Rev. **55**, 526 (1939).
[25] http://www.stabilaser.dk.
[26] T. Talvard, P. G. Westergaard, M. V. DePalatis, N. F. Mortensen, M. Drewsen, B. Gøth, and J. Hald, Opt. Express **25**, 2259 (2017).
[27] W. R. Johnson, *Atomic Structure Theory* (Springer, Berlin, 2007).
[28] F. Kurth, T. Gudjons, B. Hilbert, T. Reisinger, G. Werth, and A. M. Mårtensson-Pendrill, Z. Phys. D **34**, 227 (1995).
[29] M. Wang, G. Audi, F. Kondev, W. Huang, S. Naimi, and X. Xu, Chin. Phys. C **41**, 030003 (2017).
[30] A. Kramida, Y. Ralchenko, and J. Reader (NIST ASD Team), NIST atomic spectra database (version 5.6.1), https://doi.org/10.18434/T4W30F (2018).
[31] P. T. Boggs, R. H. Byrd, and R. B. Schnabel, SIAM J. Sci. Stat. Comput. **8**, 1052 (1987).
[32] See Supplemental Material at http://link.aps.org/supplemental/10.1103/PhysRevLett.125.123003 for details regarding the calculation of the bounds and for a discussion on the impact of isotope mass uncertainties, which includes Refs. [33–39].
[33] I. Counts, J. Hur, D. P. A. Craik, H. Jeon, C. Leung, J. Berengut, A. Geddes, A. Kawasaki, W. Jhe, and V. Vuletić, preceding Letter, Phys. Rev. Lett. **125**, 123002 (2020).
[34] J. C. Berengut, C. Delaunay, A. Geddes, and Y. Soreq, arXiv:2005.06144.
[35] V. A. Dzuba, V. V. Flambaum, P. G. Silvestrov, and O. P. Sushkov, J. Phys. B **18**, 597 (1985).
[36] E. V. Kahl and J. C. Berengut, Comput. Phys. Commun. **238**, 232 (2019).
[37] J. C. Berengut, V. A. Dzuba, and V. V. Flambaum, Phys. Rev. A **68**, 022502 (2003).
[38] P. Villemoes, A. Arnesen, F. Heijkenskjold, and A. Wannstrom, J. Phys. B **26**, 4289 (1993).
[39] D. Hucul, J. E. Christensen, E. R. Hudson, and W. C. Campbell, Phys. Rev. Lett. **119**, 100501 (2017).
[40] V. V. Flambaum, A. J. Geddes, and A. V. Viatkina, Phys. Rev. A **97**, 032510 (2018).
[41] M. Höcker, R. Rana, and E. G. Myers, Phys. Rev. A **88**, 052502 (2013).
[42] E. G. Myers, Atoms **7**, 37 (2019).
[43] A. Rischka, H. Cakir, M. Door, P. Filianin, Z. Harman, W. J. Huang, P. Indelicato, C. H. Keitel, C. M. König, K. Kromer, M. Müller, Y. N. Novikov, R. X. Schüssler, C. Schweiger, S. Eliseev, and K. Blaum, Phys. Rev. Lett. **124**, 113001 (2020).
[44] W. M. Yao *et al.* (Particle Data Group), J. Phys. G **33**, 1 (2006).
[45] J. A. Grifols and E. Masso, Phys. Lett. B **173**, 237 (1986).
[46] J. A. Grifols, E. Masso, and S. Peris, Mod. Phys. Lett. A **04**, 311 (1989).
[47] J. Redondo and G. Raffelt, J. Cosmol. Astropart. Phys. 08 (2013) 034.
[48] E. Hardy and R. Lasenby, J. High Energy Phys. 02 (2017) 033.
[49] C. Patrignani *et al.* (Particle Data Group), Chin. Phys. C **40**, 100001 (2016).
[50] D. Hanneke, S. F. Hoogerheide, and G. Gabrielse, Phys. Rev. A **83**, 052122 (2011).
[51] R. Barbieri and T. E. O. Ericson, Phys. Lett. **57B**, 270 (1975).
[52] H. Leeb and J. Schmiedmayer, Phys. Rev. Lett. **68**, 1472 (1992).
[53] Yu. N. Pokotilovski, Phys. At. Nucl. **69**, 924 (2006).
[54] V. V. Nesvizhevsky, G. Pignol, and K. V. Protasov, Phys. Rev. D **77**, 034020 (2008).
[55] D. Banerjee *et al.* (NA64 Collaboration), Phys. Rev. D **101**, 071101(R) (2020).
[56] D. Banerjee, V. E. Burtsev, A. G. Chumakov, D. Cooke, P. Crivelli *et al.* (NA64 Collaboration), Phys. Rev. Lett. **120**, 231802 (2018).
[57] J. Batley *et al.* (NA48/2 Collaboration), Phys. Lett. B **746**, 178 (2015).
[58] J. L. Feng, T. M. P. Tait, and C. B. Verhaaren, Phys. Rev. D **102**, 036016 (2020).
[59] U. D. Jentschura and I. Nándori, Phys. Rev. A **97**, 042502 (2018).
[60] M. Bordag, U. Mohideen, and V. M. Mostepanenko, Phys. Rep. **353**, 1 (2001).
[61] M. Bordag, G. L. Klimchitskaya, U. Mohideen, and V. M. Mostepanenko, Int. Ser. Monogr. Phys. **145**, 1 (2009), https://inspirehep.net/literature/841474.
[62] P. Müller, K. König, P. Imgram, J. Krämer, and W. Nörtershäuser, Collinear laser spectroscopy of Ca^+: Solving the field-shift puzzle of the $4s\,^2S_{1/2}$-$4p\,^2P_{1/2,3/2}$ transitions (to be published).
[63] C. Shi, F. Gebert, C. Gorges, S. Kaufmann, W. Nörtershäuser, B. K. Sahoo, A. Surzhykov, V. A. Yerokhin, J. C. Berengut, F. Wolf, J. C. Heip, and P. O. Schmidt, Appl. Phys. B **123**, 2 (2017).
[64] A. Kramida, At. Data Nucl. Data Tables **133**, 101322 (2020).